Soft Matter

RSC Publishing

PAPER

View Article Online
View Journal | View Issue

Cite this: *Soft Matter*, 2013, **9**, 4036

Switching preorganization and thermoresponsive behavior of a water-soluble polymer *via* light-tunable hydrogen bonding

Fen Wu, Xianghua Tang, Lei Guo, Ke Yang and Yuanli Cai*

Received 3rd January 2013
Accepted 5th February 2013

DOI: 10.1039/c3sm00020f

www.rsc.org/softmatter

We report a general approach that can switch preorganization and thermoresponsive behaviour of a water-soluble polymer *via* light-tuned hydrogen bonding (H-bonding) "dimerization" or "polymerisation". To this end, well-defined copolymers of 2-hydroxy-3-(4-hydroxyiminomethyl)-phenoxypropyl methacrylate with oligo(ethylene glycol) methacrylate (OEGMA) were synthesized *via* RAFT copolymerisation of 3-(4-formylphenoxy)-2-hydroxypropyl methacrylate with OEGMA under visible light irradiation at 25 °C and fully converting the aldehyde groups into the targeted oxime groups. Photoisomerization and stability of these oxime groups, and the effect of oxime configurations on preorganization and thermoresponsive behaviour were studied using dynamic light scattering and temperature-variable ^{1}H NMR. The results demonstrated that photoisomerization of *E*-oximes equilibrated at 76% *Z*-type formation. These oxime groups were stable against heating at 80 °C in water for 8 h. Moreover, the self-restrained H-bonding "dimerization" of *E*-oximes led to the small-sized micelles with negligible hysteresis, while the extensible H-bonding "polymerisation" of *Z*-type ones led to the enlarged micelles with remarkable hysteresis.

Introduction

Thermoresponsive water-soluble polymers have become an increasingly important class of materials that are quite promising in emerging biomedical and intelligent materials.[1–3] These smart polymers can adapt to surrounding aqueous environments and undergo an abrupt phase transition in response to a small change in temperature. Introducing photosensitivity into water-soluble polymers may induce well-defined self-assembly *via* preorganization and/or thermoresponsive micellization in water that is crucial for bio-/nano-related applications.[4–7] To date, reversible photoisomerization of *trans*-/*cis*-azobenzene[8,9] or spiropyran-merocyanine,[10,11] and the irreversible cleavage of photosensitive groups[12,13] have been employed for this purpose. These reported thermoresponsive behaviors are based on the light-tuned hydrophilicity of such water-soluble polymers.[4–15]

Actually, light-induced rearrangements of hydrogen bonding commonly proceed inside the precisely-preorganized photosensitive proteins. For example, during the light-powered proton pumping of the proteorhodopsin inside the *halobacteria* purple membrane, all-*trans* retinyl isomerizes into 13-*cis* on sunlight irradiation, which induces the transportation of imino protons neighboring retinyl outwardly *via chain-like* hydrogen bonding rearrangements.[16,17] However, to the best of our awareness, switching preorganization or thermoresponsive behavior of a water-soluble polymer *via* light-tuned hydrogen bonding inside or between the polymer chains is unprecedented. Clearly, exploring new approaches that can switch preorganization and thermoresponsive behavior of a water-soluble polymer *via* the light-tuned hydrogen bonding is important, but also quite challenging to date.

As is well known, adjusting the configuration may change the hydrogen bonding of organic compounds. For example, *E*-oximes are interlinked *via self-restrained* hydrogen bonding (H-bonding) "dimerization", whereas *Z*-type ones are interlinked *via chain-like* H-bonding "polymerisation",[18] which brings about strikingly different melting points of benzaldoxime from 35 °C (*E*-type) to 130 °C (*Z*-type)[19,20] or 4-methoxybenzaldoxime from 63 °C (*E*-type) to 132 °C (*Z*-type).[21,22] Moreover, these oximes interconvert between *E*-/*Z*-configurations upon UV irradiation or heating.[20] Thus it is reasonable to envisage that introducing such tunable hydrogen bonding into a water-soluble polymer inevitably gives rise to the tunable association of the polymer chains in water thus leading to the changes in the thermoresponsive behavior, because of the variable "dimerization" or "polymerisation" inside or between polymer chains as illustrated in Fig. 1.

Herein we report a general approach that can readily switch the preorganization and thermoresponsive behavior of water-soluble polymers *via* light-tuned hydrogen bonding of oxime groups (Fig. 1). To this end, well-defined random copolymers of

Jiangsu Key Laboratory of Advanced Functional Polymer Design and Application, Department of Polymer Science and Engineering, College of Chemistry, Chemical Engineering and Materials Science, Soochow University, Suzhou 215123, China. E-mail: ylcai@suda.edu.cn; Fax: +86-512-6588-4419; Tel: +86-512-6588-4419

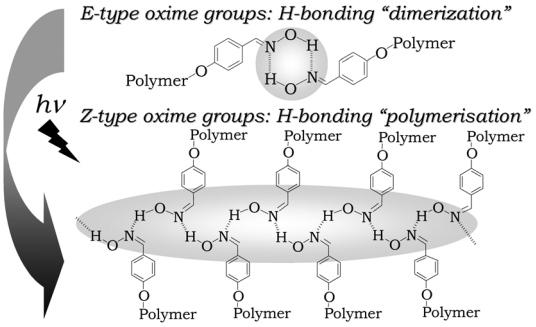

Fig. 1 Schematic illustration for the H-bonding "dimerization" (*E*-oximes) or "polymerisation" (*Z*-oximes) inside or between the polymer chains that can be switched *via* the isomerization of oxime groups upon UV irradiation.

2-hydroxy-3-(4-hydroxyiminomethyl)phenoxypropyl methacrylate with oligo(ethylene glycol) methacrylate [P(HHPPMA-*ran*-OEGMA)] were synthesized *via* RAFT copolymerisation of 3-(4-formylphenoxy)-2-hydroxypropyl methacrylate (FPHPMA) and OEGMA under visible light irradiation at 25 °C,[23–26] and then the aldehyde groups were fully converted into the targeted oxime groups *via* reacting with hydroxylamine. Photoisomerization and stability of their oxime groups, and the effect of *E*-/*Z*-oxime configurations on the preorganization and thermoresponsive behavior were studied by dynamic light scattering and temperature-variable ^{1}H NMR.

Experimental section

Materials

Glycidyl methacrylate (GMA) and oligo(ethylene glycol) monomethyl ether methacrylate (OEGMA, $M_n = 475$ g mol^{-1}, $M_w/M_n = 1.03$) were purchased from Aldrich. OEGMA was passed through a basic alumina column to remove inhibitor; GMA was dried over 4 Å molecular sieves overnight and then distilled under reduced pressure. Both monomers were stored at −20 °C prior to use. 2-Cyanoprop-2-yl(4-fluoro)dithiobenzoate (CPFDB) chain transfer agent was synthesized according to the reported procedures.[27] (2,4,6-Trimethylbenzoyl)diphenylphosphine oxide (TPO, 97%) photoinitiator was purchased from Runtec Co., 4-hydroxybenzaldehyde was purchased from Langrui Co., and hydroxylamine hydrochloride ($HONH_2HCl$), chloroform-d, dimethylsulfoxide-d_6 (DMSO-d_6) and heavy water (D_2O) were purchased from Aldrich; these agents were used as received. Water was freshly deionized to $R > 18.25$ MΩ cm prior to DLS studies.

Light source

A 500 W mercury lamp emitting separately at $\lambda = 254$, 302, 313, 365, 405, 436, 545, and 577 nm was directly employed for the photoisomerization of the oxime groups. After filtering UV light using JB400 filters, this light was used to activate the RAFT process.

Synthesis of FPHPMA

GMA (17.48 g, 0.123 mol), 4-hydroxybenzaldehyde (15.00 g, 0.123 mol), tetramethylammonium bromide (0.947 g, 0.062 mol) and ethanol (40.0 mL) were charged in a dried flask. The solution was refluxed in a nitrogen gas atmosphere at 85 °C for 10 h. The mixture was concentrated by rotary evaporation, dissolved in chloroform (40 mL), and subsequently washed using a 4.0 wt% NaOH (aq.), saturated NaCl (aq.) and finally water until it was neutralized. The solution was dried over anhydrous $MgSO_4$. After being filtered, the solvent was removed under reduced pressure. The crude product was recrystallized from ethyl ether at −18 °C and dried in vacuum at 25 °C to give a white solid product. Weight: 20.10 g and yield: 60%. ^{1}H NMR (δ, in $CDCl_3$): 9.87 ppm (1H, C*H*O); 7.00, 7.84 ppm (4H, C_6H_4); 6.14, 5.60 ppm (2H, CH_2=C(CH_3)); 4.31–4.37 ppm (2H, COOCH_2CH); 4.13 ppm (2H, CH(OH)CH_2O); 2.74 ppm (1H, CH_2CH(O*H*)CH_2); 1.93 ppm (3H, CH_2=C(CH_3)).

RAFT polymerisation under visible light radiation at 25 °C

Typically, FPHPMA (1.00 g, 3.78 mmol), OEGMA (1.796 g, 3.78 mmol), CPFDB (12.7 mg, 0.058 mmol), TPO (6.0 mg, 0.017 mmol) and DMF (1.87 g) were charged in a 25 mL flask. The flask was capped with rubber septa and then immersed in a thermostatic water bath at 25 °C. The solution was deoxygenated by purging with nitrogen gas for 30 min, and irradiated with mild visible light at $I_{420nm} = 200$ μW cm^{-2} at 25 °C for 90 min. The light intensity was measured using a UV-A radiometer fitted with a 420 nm detector. This polymerisation was quenched on exposure to air and adding traces of hydroquinone inhibitor. One portion of the solution was directly diluted in chloroform-d. Based on ^{1}H NMR studies, 49.0% FPHPMA and 47.5% OEGMA monomers were polymerized. The polymer was precipitated from a large excess of ethyl ether under stirring at 25 °C. After being filtered, the solid polymer was washed with ethyl ether 3 times and dried in a vacuum oven at 25 °C for 24 h. Weight: 1.175 g and yield: 87.5%; ^{1}H NMR: $M_n = 23.1$ kg mol^{-1}, P($FPHPMA_{31}$-*ran*-$OEGMA_{31}$); GPC: $M_n = 45.3$ kg mol^{-1} and $M_w/M_n = 1.15$.

Synthesis of P(HHPPMA-*ran*-OEGMA) copolymers

Typically, P($FPHPMA_{31}$-*ran*-$OEGMA_{31}$) (^{1}H NMR: $M_n = 23.1$ kg mol^{-1}; GPC: $M_n = 45.3$ kg mol^{-1}, $M_w/M_n = 1.15$; 3.000 g, 4.03 mmol aldehyde groups) and $HONH_2HCl$ (1.126 g, 16.12 mmol) were dissolved in DMF (15 mL) in a 25 mL flask. NaOH (8.1 mol L^{-1} in water, 2.0 mL) was added dropwise into this flask under stirring at 25 °C, and further stirred overnight at 25 °C. The copolymer was purified by dialysis from water at pH 8.0 (triethylamine added, measured by a PHS-3C digital pH meter) for 2 days and freeze-dried overnight. The solids were dissolved in DMSO-d_6 to assess the conversion of aldehydes into oximes using ^{1}H NMR.

Photoisomerization of oxime groups

Typically, $PHHPPMA_{59}$ (^{1}H NMR: $M_n = 16.4$ kg mol^{-1}; GPC: $M_n = 30.0$ kg mol^{-1}, $M_w/M_n = 1.13$; 0.100 g, 0.36 mmol of oxime groups) was dissolved in anhydrous THF (10.0 mL) in a 25 mL quartz flask. This flask was capped with rubber septa, and then immersed in a thermostatic water bath at 25 °C. The solution was deoxygenated by purging nitrogen gas for 40 min and

irradiated with UV light at $I_{365nm} = 700$ μW cm^{-2}, as measured using a UV-A radiometer fitted with a 365 nm detector. The samples were collected at predetermined intervals. The degrees of isomerization were assessed by ^{1}H NMR. The procedures for the photoisomerization of the copolymers were the same as mentioned above and were also conducted at the oxime concentrations of 36.0 mmol L^{-1}.

Gel Permeation Chromatography (GPC)

GPC measurements were performed on a PL-GPC 120 integrated system fitted with a refractive index detector. The columns (30 cm PL gel Mixed-D, 2 in series) were eluted with DMF that contained 0.01 mol L^{-1} LiBr. A series of near-monodisperse polystyrene (PS) standards (0.580–300.0 kg mol^{-1}) were used for calibration. All calibration and analysis were performed at 80 °C and a flow rate of 1.0 mL min^{-1}.

Dynamic Light Scattering (DLS)

DLS studies were performed on a BI-200SM Brookhaven setup fitted with a 100 mW solid-state laser at $\lambda_{em} = 532$ nm, a BI-200SM goniometer and a BI-9000 digital correlator. The laser was adjusted to 10.0 mW. Temperature was controlled using a BI-TCD controller. Typically, P(HHPPMA$_{31}$-*ran*-OEGMA$_{31}$) (10.0 mg) was dissolved in water (10.0 mL) in a 50 mL flask and stirred overnight at 5 °C. The dust was removed by passing through a 0.45 μm filter at 5 °C. The solution was moved to a DLS cuvette, placed in a sample cell, and kept at 8 °C for 20 min. The solution was heated at 1.0 °C min^{-1} up to a predetermined temperature and stabilized for 5 min. The scattered light was collected at 90° for 5 min. The hydrodynamic diameters (D_h) were calculated using cumulants analysis in CONTIN routine. All data were averaged over three times.

Temperature-variable ^{1}H NMR

^{1}H NMR studies were performed on a 400 MHz Bruker AV-400 NMR spectrometer fitted with a temperature controller. The polymer sample (4.0 mg) was dissolved in D_2O (4.0 mL) and stirred overnight at 5 °C. The dust was removed using a 0.45 μm filter. The solution (0.5 mL) was moved to a NMR cuvette. After being stabilized at 20 °C for 2 h, the solution was heated at 1.0 °C min^{-1} to a predetermined temperature and stabilized for 5 min. The ^{1}H NMR spectrum was recorded under scanning 32 times.

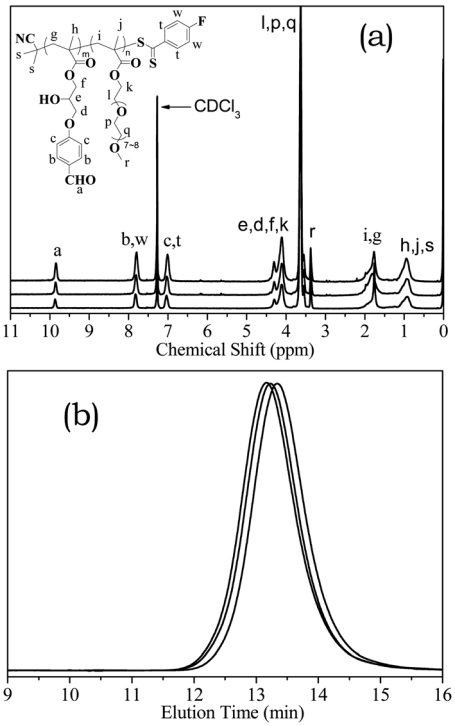

Fig. 2 (a) ^{1}H NMR spectra (from upper to bottom) and (b) GPC traces (from right to left) of P(FPHPMA$_{41}$-*ran*-OEGMA$_{19}$), P(FPHPMA$_{36}$-*ran*-OEGMA$_{25}$) and P(FPHPMA$_{31}$-*ran*-OEGMA$_{31}$) copolymers.

Results and discussion

Synthesis of P(HHPPMA-*ran*-OEGMA) copolymers

Firstly, P(FPHPMA-*ran*-OEGMA) copolymers were synthesized *via* RAFT copolymerisation of FPHPMA and OEGMA under visible light radiation at 25 °C. As shown in Fig. 2a, except the signal of C*H*Cl$_3$ in CDCl$_3$, the signals of C*H*$_2$=CCH$_3$ (monomers) at $\delta = 5.56$ ppm and other impurities could not be detected, suggesting that the monomers and other impurities were removed. Moreover, the integral ratios were consistent with the assigned proton ratios of copolymers, suggesting intact structures of the copolymers. Although the signals of C_6H_4F (t and w, in CPFDB chain-ends) overlapped with the C_6H_4CHO signals (b and c, in FPHPMA units) at $\delta = 7.0$–7.8 ppm, the C_6H_4CHO signal (a) at $\delta = 9.8$ ppm was quite clear. Moreover, the signals of protons e, d, f, and k in both units were detected at $\delta = 3.8$–4.5 ppm. Accordingly, the apparent individual (DP_{FPHPMA}, DP_{OEGMA}) and the overall (DP) degrees of polymerisation were assessed according to eqn (1)–(3).

$$DP_{FPHPMA} = \frac{2I_a}{I_{b+w} - 2I_a} \quad (1)$$

$$\frac{DP_{OEGMA}}{DP_{FPHPMA}} = \frac{I_{e+d+f+k} - 5I_a}{2I_a} \quad (2)$$

$$DP = DP_{FPHPMA} + DP_{OEGMA} \quad (3)$$

As shown in Fig. 2b, the GPC traces were unimodal and symmetrical, and slightly shifted to the higher molecular weight side on the increase of OEGMA fractions, most presumably due to the higher molecular weight and more significant steric effect of OEGMA than FPHPMA units. In order to figure out the effect of oxime configurations on preorganization and thermoresponsive behavior, the copolymers whose FPHPMA fractions over 50% were selected as the parent copolymers. As shown in Table 1, the selected parent copolymers were well-defined with almost the same chain lengths (DP = 61 ± 1) at narrow molecular weight distributions (M_w/M_n = 1.12–1.15) but different compositions.

Table 1 Structure parameters of aldehyde-functional P(FPHPMA-*ran*-OEGMA) selected for the synthesis of the oxime-functional copolymers

No.	$M_{n,GPC}$ (kg mol^{-1})	M_w/M_n	$M_{n,^1H\ NMR}$ (kg mol^{-1})	DP[a]	Composition[a]
1	43.4	1.12	20.1	60	P(FPHPMA$_{41}$-*ran*-OEGMA$_{19}$)
2	44.8	1.15	21.3	61	P(FPHPMA$_{36}$-*ran*-OEGMA$_{25}$)
3	45.3	1.15	23.1	62	P(FPHPMA$_{31}$-*ran*-OEGMA$_{31}$)

[a] Overall degrees of polymerisation (DP) and compositions were assessed by ^{1}H NMR studies.

The targeted P(HHPPMA-*ran*-OEGMA) copolymers were achieved *via* adding NaOH (aq.) to DMF solution of P(FPHPMA-*ran*-OEGMA) and $HONH_2HCl$, and then stirring at 25 °C for 6 h. As shown in Fig. 3, the C_6H_4CHO signal at δ = 9.8 ppm disappeared, and the C_6H_4CH=NOH signals at δ = 8.05, 7.93, 7.50, 7.29, and 6.95 ppm were clearly detectable. The proton signals of impurities that were possibly caused by the side reactions were not detectable. Moreover, $I_{8.05+7.29} : I_{7.50+7.93} : I_{6.95}$ was assessed to be 1 : 2 : 2, within analysis errors. These results suggested that their aldehyde groups were fully converted into the targeted oxime groups, *i.e.* the parent copolymers were converted into the targeted copolymers.

More importantly, the integral ratios of $I_{8.05} : I_{7.29}$ and $I_{7.50} : I_{7.93}$ were constant at 9 : 1, suggesting that the oxime configuration ratios remained at the same value of $[E]/[Z]$ = 90 : 10. These *E*/*Z*-oxime ratios were in good agreement with those of the benzaldoxime compound synthesized *via* reaction of benzaldehyde with $HONH_2HCl$ in water–ethanol on adding sodium acetate at room temperature.[28]

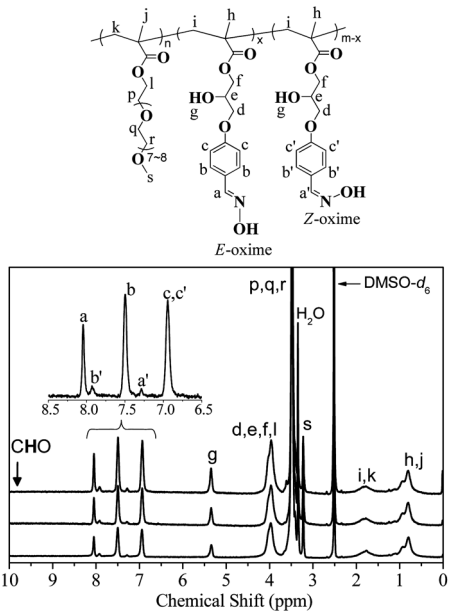

Fig. 3 ^{1}H NMR spectra of P(HHPPMA$_{41}$-*ran*-OEGMA$_{19}$), P(HHPPMA$_{36}$-*ran*-OEGMA$_{25}$), and P(HHPPMA$_{31}$-*ran*-OEGMA$_{31}$) in DMSO-d$_6$ (from top to bottom).

Photoisomerization of oxime groups

The photoisomerization proceeded *via* the UV irradiation of the copolymers at the same oxime concentrations of 36.0 mmol L^{-1} in a nitrogen gas atmosphere at 25 °C. As shown in Fig. 4a, the signals a and b in *E*-C_6H_4CH=NOH were gradually attenuated, while the signals a′ and b′ in *Z*-C_6H_4CH=NOH were gradually enhanced upon irradiation with UV light, suggesting that *E*-oximes gradually isomerized to *Z*-type ones. Moreover, the signals of impurities possibly caused by the rearrangement or cycloaddition of oximes[20] could not be detected under such conditions.

As shown in Fig. 4b, this photoisomerization equilibrated at 76% *Z*-type formation. More specifically, the photoisomerization of *E*-type oxime groups was clearly more rapid in the homopolymer chains than in the copolymer chains, which were most presumably caused by the light-screening effect of OEGMA units that were adjacent to HHPPMA units.

Stability of oxime groups against heating in aqueous media

Clearly, excellent stability of these oxime groups against heating in water was crucial because the thermoresponsive behavior of such water-soluble polymers should be studied in the heated water. Accordingly, the stability of oxime groups against heating in aqueous media was studied by sequentially adding heavy water to the copolymer solutions in DMSO-d$_6$ and heating up to 80 °C, and then analyzing using ^{1}H NMR.

As shown in Fig. 5a, for P(HHPPMA$_{31}$-*ran*-OEGMA$_{31}$) ($[E] : [Z]$ = 90 : 10, in DMSO-d$_6$), although the proton signal g in $CH_2CH(OH)CH_2$ disappeared upon adding D_2O, the other

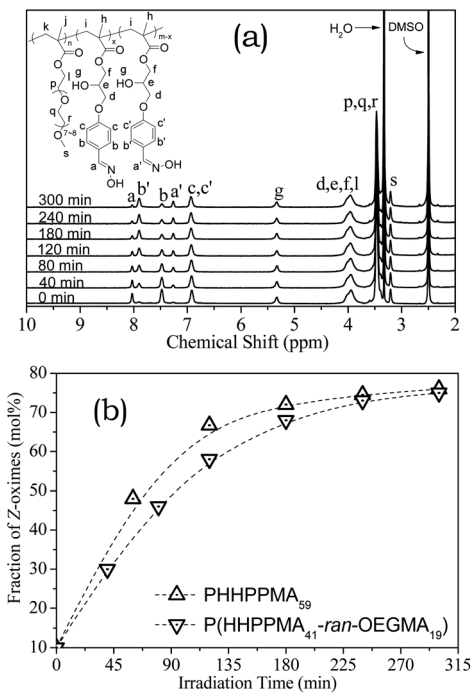

Fig. 4 (a) The evolution of the ^{1}H NMR spectrum of P(HHPPMA$_{41}$-*ran*-OEGMA$_{19}$) upon UV irradiation at 25 °C and (b) the kinetic curves for photoisomerization of oxime groups.

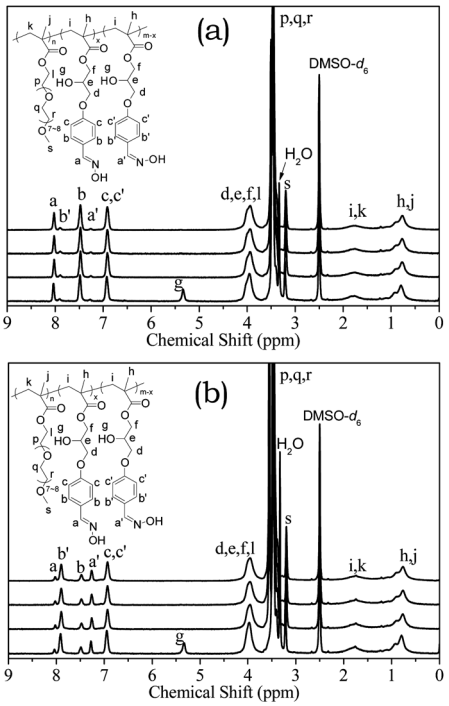

Fig. 5 ^{1}H NMR spectra of P(HHPPMA$_{31}$-*ran*-OEGMA$_{31}$) at $[E]:[Z] = 90:10$ (a) and 26 : 74 (b). From bottom to top: in DMSO-d_6 at 20 °C; in DMSO-d_6 and D_2O (1 : 1 v/v) at 20 °C; in DMSO-d_6 and D_2O (1 : 1 v/v) at 80 °C for 4 h; and in DMSO-d_6 and D_2O (1 : 1 v/v) at 80 °C for 8 h.

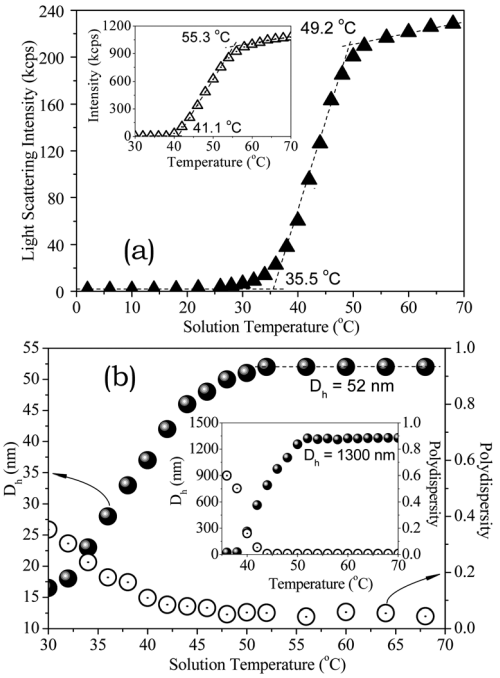

Fig. 6 The evolution of (a) light scattering intensity, (b) hydrodynamic diameter (D_h, solid) and polydispersity (μ_2/Γ^2, hollow) of P(HHPPMA$_{31}$-*ran*-OEGMA$_{31}$) ($[E]:[Z] = 90:10$, 1.0 mg mL^{-1} in H_2O) upon heating. Inset: those of the corresponding aldehyde-functional parent copolymer.

signals of this copolymer were fully detectable. These results suggested that the copolymer molecularly dissolved in DMSO-d_6–D_2O media. Moreover, these proton signals did not change upon heating up to 80 °C for 4 or 8 h, as indicated by the undetectable additional side-reaction signals. These results demonstrated that both *E*- and *Z*-type oxime groups were stable against heating in water.

As shown in Fig. 5b, for the *Z*-isomerized copolymer at $[E]:[Z] = 26:74$, the proton signals of the copolymer also remained the same after heating the aqueous solution up to 80 °C for 4 or 8 h. These results suggested that both *E*- and *Z*-type oxime groups were stable under such heating conditions. This excellent stability facilitated the studies on the thermoresponsive behavior of such copolymers in the heated water.

Preorganization and thermoresponsive behavior of oxime-functional P(HHPPMA-*ran*-OEGMA)

Dynamic light scattering (DLS) was employed to figure out the preorganization and thermoresponsive behavior of such water-soluble polymers in aqueous media. In order to elucidate the hydrogen bonding effect of the oxime groups, the aldehyde-functional parent copolymers were also studied for comparison. Firstly, P(HHPPMA$_{31}$-*ran*-OEGMA$_{31}$) at $[E]:[Z] = 90:10$ (1.0 mg mL^{-1} in water) was selected for DLS studies.

As shown in Fig. 6a, the light scattering intensity remained below 1.0 kcps upon heating from 2 °C to 30 °C, suggesting that the copolymer molecularly dissolved in water. Further heating up to 35.5 °C led to a sharp increase of light scattering intensity, suggesting that the copolymer had started to phase-separate from water. This critical temperature was the so-called cloud point (CP). Interestingly, although the oxime groups were more water-soluble than aldehyde groups, converting these aldehyde groups into water-soluble oxime groups brought about the remarkable CP-lowering down to $\Delta T = -5.6$ °C. These results demonstrated that the hydrogen bonding of oxime groups effectively enhanced the association of these polymer chains, thus promoting the phase transition in response to heating.

Further heating the solution above 49 °C resulted in a second leveling-off of the light scattering intensity. This copolymer self-assembled into micelles with the intensity-average hydrodynamic diameter $D_h = 52$ nm and low polydispersity $\mu_2/\Gamma^2 = 0.05$ (Fig. 6b). Moreover, these micelles were remarkably smaller than the irregular aggregates of the corresponding aldehyde-functional parent copolymer ($D_h = 1300$ nm). Moreover, this critical temperature was clearly lower than that of the parent copolymer, down to $\Delta T = -6.1$ °C. Thus it was named as the critical temperature for the formation of compact micelles (T_c).

As summarized in Table 2, at the same oxime configuration ratios at $[E]:[Z] = 90:10$, increasing [HHPPMA] : [OEGMA] from 31 : 31 to 36 : 25 led to the remarkable CP-decrease from 35.5 °C down to 18 °C, and also T_c from 49.2 °C to 29.2 °C. The size of micelles slightly decreased from $D_h = 52$ nm down to 48 nm.

Further increasing [HHPPMA] : [OEGMA] to 41 : 19 resulted in the copolymer already associated or preorganized into micelles at $D_h = 36$ nm and a low polydispersity $\mu_2/\Gamma^2 = 0.06$ prior to heating the aqueous solution, even at a low temperature of 2 °C, which led to a high light scattering intensity of

Table 2 Critical temperatures (including CP and T_c), light scattering intensity of 1.0 mg mL^{-1} P(HHPPMA-*ran*-OEGMA) ([*E*] : [*Z*] = 90 : 10) in water and D_h of their compact micelles over T_c

Copolymer	CP (°C)	T_c (°C)	Intensity (kcps)	D_h (nm)
P(HHPPMA$_{41}$-*ran*-OEGMA$_{19}$)	NA[a]	NA[a]	121	34
P(HHPPMA$_{36}$-*ran*-OEGMA$_{25}$)	18.6	29.1	174	48
P(HHPPMA$_{31}$-*ran*-OEGMA$_{31}$)	35.5	49.2	228	52

[a] NA: not applicable.

66.6 kcps. The micelles just slightly shrank on heating from 2 to 15 °C. More importantly, these micelles remained at the same size at D_h = 34 nm, *i.e.* the coacervation could not be detected on further heating from 15 °C to 40 °C (see Fig. 7). These results suggested that these compact micelles were quite stable against heating around the physiological temperature of 37 °C. Accordingly, it could be concluded that this water-soluble copolymer exhibited a well-defined preorganization character in water. The fascinating stability of these micelles is certainly desirable for the potential applications in emerging biomedical or nano-structured materials.

The oxime-configuration effect on preorganization and thermoresponsive behavior

As shown in Fig. 7a, for P(HHPPMA$_{41}$-*ran*-OEGMA$_{19}$) (1.0 mg mL^{-1} in water), although [*E*] : [*Z*] increased from 90 : 10 to 58 : 42 and finally to 26 : 74, the light scattering intensity maintained the same evolving tendency on heating. Either coacervation or dissociation of micelles were not observed upon heating from 2 °C to 40 °C. These results demonstrated that the micelles maintained the excellent stability around the physiological temperature of 37 °C over a wide range of *E*-/*Z*-configurations. More importantly, the compact micelles enlarged from D_h = 34 nm to D_h = 43 nm and finally to D_h = 61 nm (Fig. 7b) on the increase of *Z*-oxime fractions, which brought about the remarkable increase of light scattering intensity upon heating to the same temperatures (Fig. 7a). These results demonstrated that *Z*-type oxime groups could enhance the intermolecular association of the polymer chains effectively during the preorganization into micelles in water, even at a low temperature of 2 °C.

In contrast, as shown in Fig. 8a, for P(HHPPMA$_{31}$-*ran*-OEGMA$_{31}$) over a wide range of [*E*] : [*Z*] = 90 : 10 to 26 : 74 (1.0 mg mL^{-1} in water), the light scattering intensity remained below 1.0 kcps on heating the solutions from 2 °C to 35.5 °C, suggesting that the copolymers were molecularly dissolved in water, rather than preorganized into micelles as observed above. Further heating led to the starting-up of phase transition at a CP = 35.5 °C, as indicated by the abrupt increase of light scattering intensity. Varying *E*-/*Z*-oxime ratios did not change the critical temperatures including CP and T_c, suggesting the negligible effect of *E*-/*Z*-oxime configurations on the hydration/dehydration behaviour.

However, as shown in Fig. 8b, the size of compact micelles clearly enlarged from D_h = 52 nm up to 60 nm and finally to 74 nm on increasing *Z*-oxime fractions from 10% to 44%, and to 74%, which brought about the remarkable increase of light scattering intensity on heating up over the critical temperatures

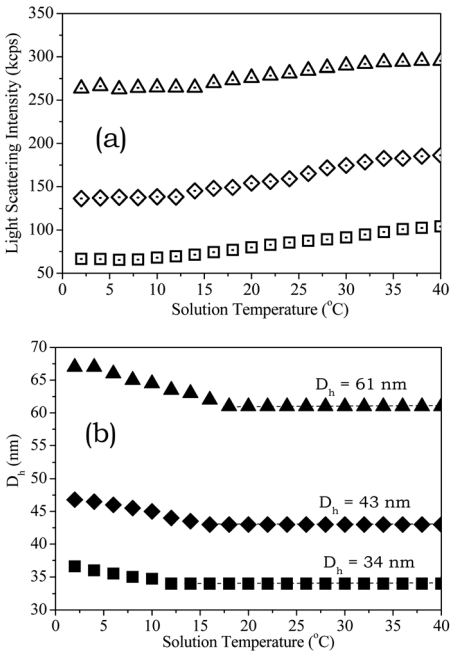

Fig. 7 The heating-induced evolution of (a) the light scattering intensity of 1.0 mg mL^{-1} P(HHPPMA$_{41}$-*ran*-OEGMA$_{19}$) copolymers in H_2O and (b) the hydrodynamic diameter (D_h) of these preorganized micelles. *E*/*Z*-oxime ratios ([*E*] :[*Z*]): 90 : 10 (triangle), 58 : 42 (diamond), and 26 : 74 (square).

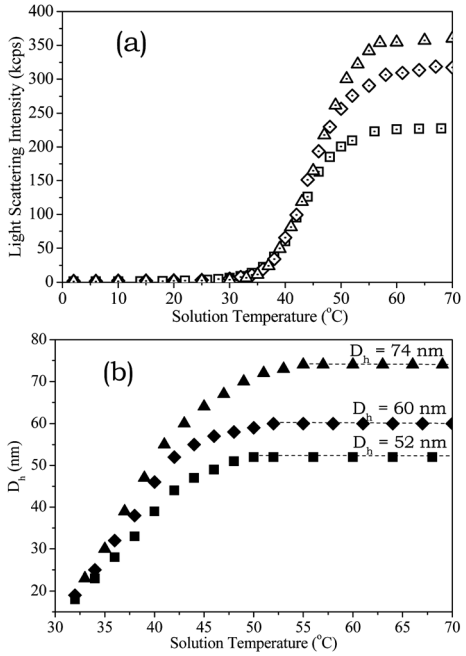

Fig. 8 The heating-induced evolution of (a) the light scattering intensity of 1.0 mg mL^{-1} P(HHPPMA$_{31}$-*ran*-OEGMA$_{31}$) copolymers in H_2O and (b) the hydrodynamic diameter (D_h) of their thermoresponsive micelles. *E*/*Z*-oxime ratios ([*E*] : [*Z*]): 90 : 10 (triangle), 56 : 44 (diamond), and 26 : 74 (square).

(Fig. 8a). This enlarging tendency of thermoresponsive micelles on the increase of *Z*-oxime fractions was in reasonably good agreement with the enlarging tendency of preorganized micelles of P(HHPPMA$_{41}$-*ran*-OEGMA$_{19}$). These results suggested that the *Z*-oxime groups could effectively enhance the intermolecular association of the polymer chains during the thermoresponsive micellization in water.

The effect of oxime configurations was further investigated using heavy water (D_2O) as a solvent. As shown in Fig. 9, varying the oxime configurations ([*E*] : [*Z*]) also resulted in the enlargement of preorganized micelles of P(HHPPMA$_{41}$-*ran*-OEGMA$_{19}$) and thermoresponsive micelles of P(HHPPMA$_{31}$-*ran*-OEGMA$_{31}$) in D_2O, which were similar to those observed in H_2O.

In contrast, on heating above T_c, light scattering intensities of D_2O solutions were lower than those of H_2O solutions due to the formation of smaller micelles in D_2O than in H_2O. More specifically, the sizes of P(HHPPMA$_{41}$-*ran*-OEGMA$_{19}$) compact micelles were at a D_h = 31 nm ([*E*] : [*Z*] = 90 : 10), 36 nm ([*E*] : [*Z*] = 58 : 42) or 45 nm ([*E*] : [*Z*] = 26 : 74) in D_2O, smaller than the corresponding micelles in H_2O (D_h = 34, 43 or 61 nm). Similarly, the sizes of P(HHPPMA$_{31}$-*ran*-OEGMA$_{31}$) compact micelles were at a D_h = 41 nm ([*E*] : [*Z*] = 90 : 10), 46 nm ([*E*] : [*Z*] = 56 : 44) or 56 nm ([*E*] : [*Z*] = 26 : 74) in D_2O, also smaller than the corresponding micelles in H_2O (D_h = 52, 60 or 74 nm). These results confirmed that varying *Z*-/*E*-oxime configurations effectively tuned the intermolecular association of the polymer chains, inside either preorganized or thermoresponsive micelles.

Clearly, the mechanism for this photosensitivity was totally different from those *via* changing the hydrophilicity of polymer chains through the reversible photoisomerization of *trans*-/*cis*-azobenzene[8,9] or spiropyran-merocyanine,[10,11] or the irreversible cleavage of photosensitive groups,[12,13] in which photoreactions changed LCST behavior which directly brought about micellization or dissociation of the polymer chains in water. In contrast, varying *Z*-/*E*-oxime ratios, in this case, switched the association of the polymer chains but without changing the LCST behavior.

^{1}H NMR evidence for thermoresponsive behavior

Temperature-variable ^{1}H NMR was employed to clarify the effect of *E*-/*Z*-oxime configurations on the thermoresponsive behavior. P(HHPPMA$_{31}$-*ran*-OEGMA$_{31}$) copolymers at [*E*] : [*Z*] = 90 : 10 and 24 : 76 (1.0 mg mL^{-1} in D_2O) were selected for this purpose.

As shown in Fig. 10a, for the copolymer at a [*E*] : [*Z*] = 90 : 10, the signals $CH_2C(CH_3)$ at δ = 0.8–1.9 ppm (polymer backbones) and $COOCH_2$ at δ = 4.1 ppm (unit spacers) gradually attenuated on heating from 21 °C to 38 °C (DLS: CP = 35.5 °C), and then remained essentially the same on further heating up to 44 °C. These results suggested that the phase transition was induced by the hydrophobic association of the less polar polymer backbones and unit spacers. However, the OC_6H_4CH═NOH signals at δ = 6.5–8.4 ppm (*E*-oxime groups) were clearly detectable on heating from 21 to 44 °C. This indicated that *E*-oxime groups remained in the hydrated state during the thermoresponsive phase transition.

In contrast, for the copolymer at a [*E*] : [*Z*] = 24 : 76 (Fig. 10b), heating the solution also resulted in dehydration of the polymer backbones and unit spacers, as indicated by attenuation of their proton signals. Similarly, the proton signals of oxime groups remained essentially the same on heating from 21 to 44 °C. However, the signals of these oxime groups were clearly weaker than those of the former (Fig. 10a). These results

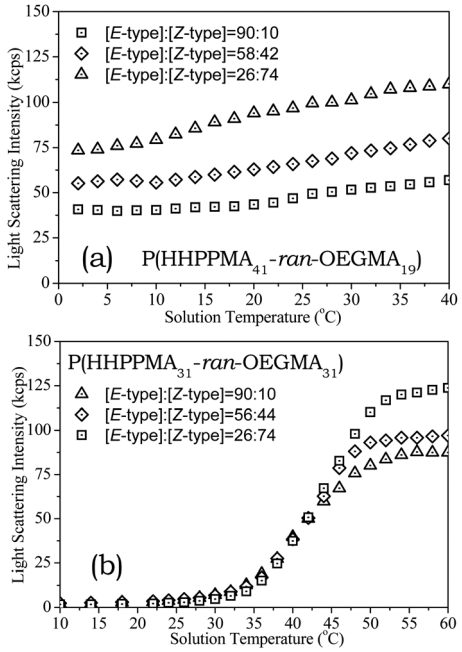

Fig. 9 The configuration-dependent evolution of the light scattering intensity of 1.0 mg mL^{-1} P(HHPPMA-*ran*-OEGMA) in D_2O on heating.

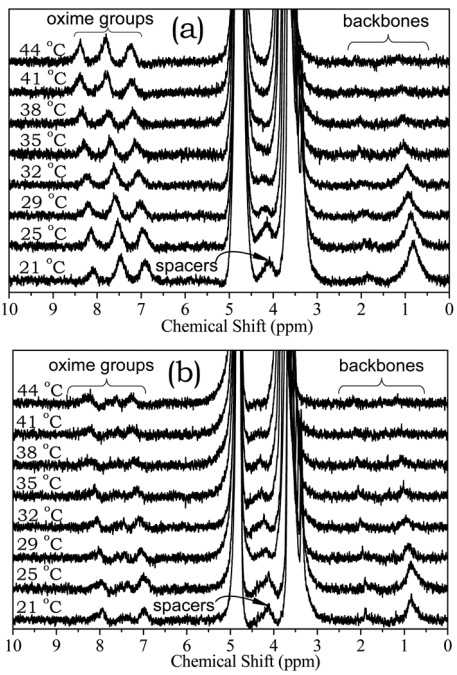

Fig. 10 ^{1}H NMR spectra evolution of P(HHPPMA$_{31}$-*ran*-OEGMA$_{31}$) at a [*E*] : [*Z*] = 90 : 10 (a) or 24 : 76 (b) (1.0 mg mL^{-1} in D_2O) on heating.

suggested that the *Z*-oxime groups were partially dehydrated, *i.e.* *Z*-oxime groups tended to be interlinked *via chain-like* H-bonding "polymerisation", which inevitably enhanced the intermolecular association of the polymer chains, thus leading to the enlarged thermoresponsive micelles.

Hydrogen bonding modulated by *E*-/*Z*-oxime configurations

As shown in Fig. 11a, for P(HHPPMA$_{31}$-*ran*-OEGMA$_{31}$) at a $[E]:[Z] = 90:10$ (1.0 mg mL^{-1} in H_2O), the cooling-induced light scattering intensity evolution was essentially overlapped with that evolved on heating, suggesting that these micelles could be dissociated and dissolved in water rapidly on cooling the heated solution. As previously observed by the groups of Lutz,[29] Li,[30] Wu[31] and our group,[32] the rapid dissociation of micelles also occurred on heating–cooling the solutions of random copolymers of OEGMA with 2-(2-methoxyethoxy)ethyl methacrylate, oligo(ethylene glycol) acrylate with 2-(5,5-dimethyl-1,3-dioxan-2-yloxy)ethyl acrylate, and pyrrolidone-based poly(meth)acrylates. It was well known that thermoresponsive phase transition of such polymers was induced mainly by the hydrophobic association of less or apolar polymer backbones and unit spacers.[29–32] It suggested the *self-restrained* H-bonding "dimerization" of *E*-oxime groups, which did not or did just slightly contribute to the intermolecular association of the polymer chains, thus leading to the small-sized micelles and the rapid dissociation of micelles or negligible hysteresis in response to cooling.

However, for the copolymer at a $[E]:[Z] = 24:76$ (Fig. 11b), the cooling-induced phase transition significantly lagged behind the heating-induced phase transition, suggesting the dissociation of these thermo-induced micelles was more energy-consuming. This hysteresis also occurred during heating–cooling the solutions of poly(*N*-isopropyl acrylamide),[33] which was caused by the intra- and intermolecular hydrogen bonding of the amides.[34–36] These results suggested the *chain-like* H-bonding "polymerisation" of *Z*-oxime groups, which effectively enhanced the intermolecular association of the polymer chains, thus leading to the enlarged micelles and remarkable hysteresis in response to cooling.

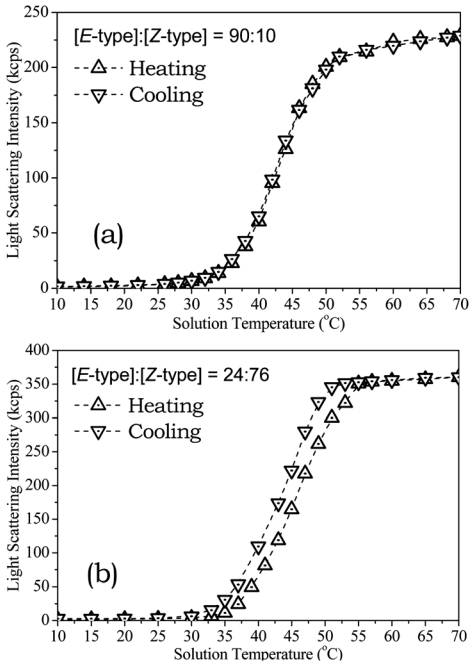

Fig. 11 The evolution of the light scattering intensity of 1.0 mg mL^{-1} P(HHPPMA$_{31}$-*ran*-OEGMA$_{31}$) in H_2O on a heating–cooling cycle.

Conclusions

This paper reported an approach that can switch preorganization and thermoresponsive behavior of a water-soluble polymer *via* light-tunable hydrogen bonding. To this end, well-defined P(HHPPMA-*ran*-OEGMA) copolymers were synthesized. The photoisomerization and stability of oxime groups, and the effect of *E*-/*Z*-oxime configurations on the preorganization and thermoresponsive behavior were studied by DLS and temperature-variable ^{1}H NMR.

The results demonstrated that the photoisomerisation of *E*-oximes into *Z*-type ones equilibrated at 76% *Z*-type formation. These oxime groups were stable in water at 80 °C for 8 h. Moreover, the self-restrained H-bonding "dimerization" of *E*-oximes led to the small-sized micelles with negligible hysteresis, whereas the extensible H-bonding "polymerization" of *Z*-oximes brought about the enlarged micelles with remarkable hysteresis. This provided a general approach toward light-tunable preorganization and thermoresponsive behavior of water-soluble polymers.

Acknowledgements

This work was supported by National Natural Science Foundation of China (20874081, 21074104 and 21274097), Priority Academic Program Development of Jiangsu Higher Education Institutions, and Scientific Research Fund of Hunan Provincial Education Department (10A116). We thank Dr Lican Lu at Xiangtan University for his assistance for the synthesis.

Notes and references

1 R. A. Álvarez-Puebla, R. Contreras-Cáceres, I. Pastoriza-Santos, J. Pérez-Juste and L. M. Liz-Marzán, *Angew. Chem., Int. Ed.*, 2009, **48**, 138.
2 M. A. C. Stuart, W. T. S. Huck, J. Genzer, M. Müller, C. Ober, M. Stamm, G. B. Sukhorukov, I. Szleifer, V. V. Tsukruk, M. Urban, F. Winnik, S. Zauscher, I. Luzinov and S. Minko, *Nat. Mater.*, 2010, **9**, 101.
3 H. Ajiro, Y. Takahashi and M. Akashi, *Macromolecules*, 2012, **45**, 2668.
4 D. Roy, J. N. Cambre and B. S. Sumerlin, *Prog. Polym. Sci.*, 2010, **35**, 278.
5 J.-M. Schumers, C.-A. Fustin and J.-F. Gohy, *Macromol. Rapid Commun.*, 2010, **31**, 1588.
6 Y. Zhao, *Macromolecules*, 2012, **45**, 3647.
7 G. Pasparakis, T. Manouras, P. Argitis and M. Vamvakaki, *Macromol. Rapid Commun.*, 2012, **33**, 183.
8 S. Dai, P. Ravi and K. C. Tam, *Soft Matter*, 2009, **5**, 2513.
9 F. D. Jochum and P. Theato, *Chem. Commun.*, 2010, **46**, 6717.

10 H. Lee, W. Wu, J. K. Oh, L. Mueller, G. Sherwood, L. Peteanu, T. Kowalewski and K. Matyjaszewski, *Angew. Chem., Int. Ed.*, 2007, **46**, 2453.
11 J. A. Nam, A. Al-Nahain, S. Lee, I. In and S. Y. Park, *Macromol. Rapid Commun.*, 2012, **33**, 1958.
12 J. Jiang, X. Tong and Y. Zhao, *J. Am. Chem. Soc.*, 2005, **127**, 8290.
13 J. Babin, M. Pelletier, M. Lepage, J.-F. Allard, D. Morris and Y. Zhao, *Angew. Chem., Int. Ed.*, 2009, **48**, 3329.
14 P. Ravi, S. L. Sin, L. H. Gan, Y. Y. Gan, K. C. Tam, X. L. Xia and X. Hu, *Polymer*, 2005, **46**, 137.
15 J. He, X. Tong and Y. Zhao, *Macromolecules*, 2009, **42**, 4845.
16 N. Hampp, *Chem. Rev.*, 2000, **100**, 1755.
17 J. M. Walter, D. Greenfield, C. Bustamante and J. Liphardt, *Proc. Natl. Acad. Sci. U. S. A.*, 2007, **104**, 2408.
18 X. Lin, W. Xu, J. Wang and C. Liu, *Chem. J. Chin. Univ.*, 2006, **27**, 897.
19 F. K. Gameron, *J. Phys. Chem.*, 1898, **2**, 409.
20 A. Padwa, *Chem. Rev.*, 1977, **77**, 37.
21 H. R. Carveth, *J. Phys. Chem.*, 1899, **3**, 437.
22 E. L. Skau and B. Saxton, *J. Phys. Chem.*, 1933, **37**, 197.
23 L. Lu, H. Zhang, N. Yang and Y. Cai, *Macromolecules*, 2006, **39**, 3770.
24 Y. Shi, G. Liu, H. Gao, L. Lu and Y. Cai, *Macromolecules*, 2009, **42**, 3917.
25 C. Cao, K. Yang, F. Wu, X. Wei, L. Lu and Y. Cai, *Macromolecules*, 2010, **43**, 9511.
26 K. Yang, X. Wei, F. Wu, C. Cao, J. Deng and Y. Cai, *Soft Matter*, 2011, **7**, 5861.
27 M. Benaglia, E. Rizzardo, A. Alberti and M. Guerra, *Macromolecules*, 2005, **38**, 3129.
28 J.-L. Boucher, M. Delaforge and D. Mansuy, *Biochemistry*, 1994, **33**, 7811.
29 J.-F. Lutz, Ö. Akdemir and A. Hoth, *J. Am. Chem. Soc.*, 2006, **128**, 13046.
30 Z. Qiao, F. Du, R. Zhang, D. Liang and Z. Li, *Macromolecules*, 2010, **43**, 6485.
31 H. Lai, G. Chen, P. Wu and Z. Li, *Soft Matter*, 2012, **8**, 2662.
32 J. Deng, Y. Shi, W. Jiang, Y. Peng, L. Lu and Y. Cai, *Macromolecules*, 2008, **41**, 3007.
33 H. Cheng, L. Shen and C. Wu, *Macromolecules*, 2006, **39**, 2325.
34 E. I. Tiktopulo, V. N. Uversky, V. B. Lushchik, S. I. Klenin, V. E. Bychkova and O. B. Ptitsyn, *Macromolecules*, 1995, **28**, 7519.
35 H. Mao, C. Li, Y. Zhang, S. Furyk, P. S. Cremer and D. E. Bergbreiter, *Macromolecules*, 2004, **37**, 1031.
36 B. Sun, Y. Lin, P. Wu and H. W. Siesler, *Macromolecules*, 2008, **41**, 1512.

